INTERNAL MIXING AND SURFACE ABUNDANCE OF [WC]-CSPN

F. HERWIG
Universität Potsdam, Germany
fherwig@astro.physik.uni-potsdam.de

Abstract. Recent advances in constructing stellar evolution models of hydrogen-deficient post-asymptotic giant branch (AGB) stars are presented. Hydrogen-deficiency can originate from mixing and subsequent convective burning of protons in the deeper layers during a thermal pulse on the post-AGB (VLTP). Dredge-up alone may also be responsible for hydrogen-deficiency of post-AGB stars. Models of the last thermal pulse on the AGB with very small envelope masses have shown efficient third dredge-up. The hydrogen content of the envelope is diluted sufficiently to produce H-deficient post-AGB stars (AFTP). Moreover, dredge-up alone may also cause H-deficiency during the Born-again phase (LTP). During the second AGB phase a convective envelope develops. A previously unknown lithium enrichment at the surface of Born-again stellar models may be used to distinguish between objects with different post-AGB evolution. The observed abundance ratios of C, O and He can be reproduced by all scenarios if an AGB starting model with inclusion of overshoot is used for the post-AGB model sequence.

An appendix is devoted to the numerical methods for models of proton capture nucleosynthesis in the He-flash convection zone during a thermal pulse.

1. Introduction

The problems of interpreting the evolutionary origin of H-deficient post-AGB stars in general and the [WC]-central stars of planetary nebulae (CSPN) in particular are described in this volume, e.g. by Koesterke and by Werner. These peculiar stars are found at positions in the HRD which correspond to post-AGB evolutionary sequences of low- and intermediate

Workshop on ‘‘Low mass Wolf-Rayet stars: origin and evolution’’, 1999, Amsterdam, to appear in ApSS, Kluwer.

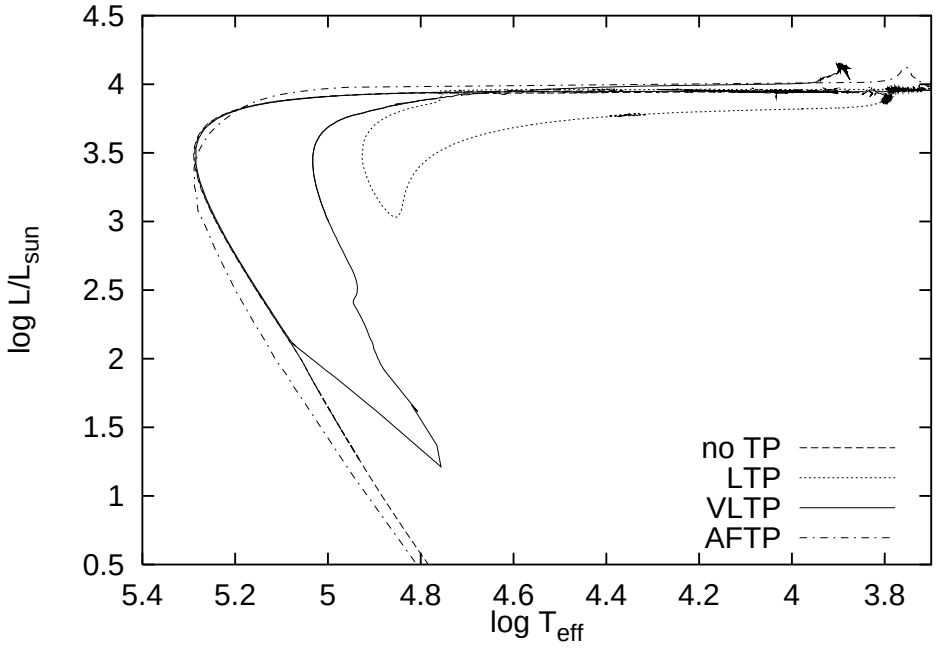

Figure 1. Evolutionary post-AGB tracks in the HRD for the four scenarios discussed in the text. The stellar mass is always $0.6M_{\odot}$.

mass stars (Fig. 1). Hydrogen is underabundant at the surface and a closer look at the various observational analysis reveals a diverse picture. H-rich stars with practically solar H-abundance, so-called hybrid objects with substantial fractions of typically more than 10% of H, H-poor with less than a few percent H and definitely H-free descendants of AGB stars like the DO-white dwarfs (WDs) have been found. With new stellar evolution models we have now identified several possibilities for the origin of H-deficiency of post-AGB stars which make different predictions for the degree of H-depletion and other elements. The recent progress in modeling these objects are either related to the mixing and simultaneous burning of the remaining envelope hydrogen or to the dredge-up (DUP). The new results are based on progenitor AGB models with overhooting.

The first possibility is the so-called *very late thermal pulse* (VLTP) and has been first suggested by Fujimoto (1977). Secondly, H-deficiency may occur after the last thermal pulse on the AGB. When the remaining envelope mass is coincidently very small at that last TP, one final dredge-up phase can significantly reduce the H-abundance and we have phrased the term *asymptotic giant branch final thermal pulse* (AFTP) for this situation. In the third case, DUP occurs during the Born-again evolution which follows

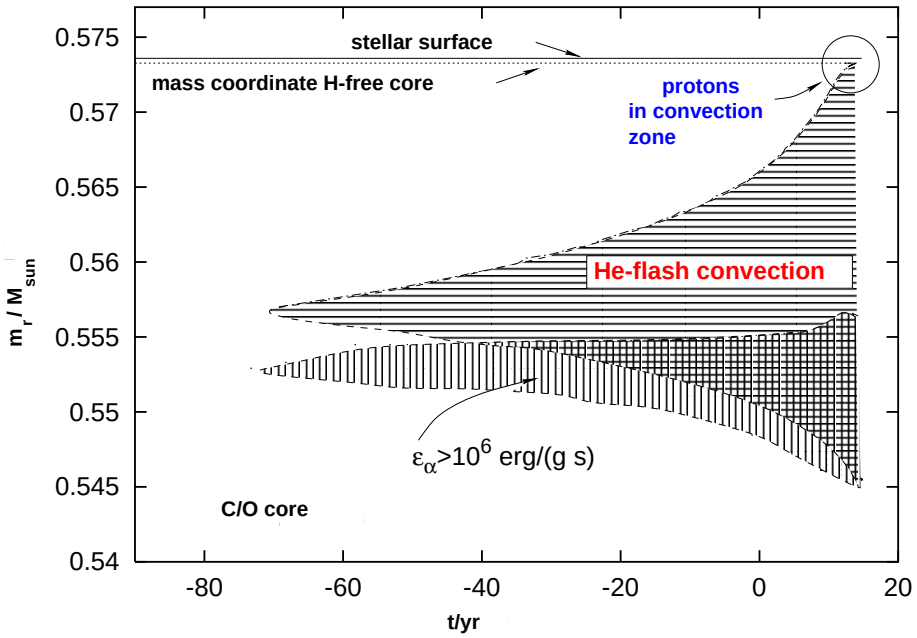

Figure 2. Internal evolution of the He-flash convection zone towards a post-AGB TP. Horizontal hatch is used for the growing He-flash convection zone. It is driven by the increasing energy production due to He-burning. The latter is marked by vertical hatches.

a post-AGB thermal pulse (either late or very late). If the model has not become H-deficient already due to combined mixing and burning during a very late thermal pulse, then it will become H-deficient due to DUP during its second AGB evolution after a *late thermal pulse* (LTP, see Blöcker, this volume).

The models presented in this paper have been computed with our stellar evolution code as described by Blöcker (1995) and extended with respect to mixing (Herwig et al. 1997) and coupled nuclear burning (Herwig et al. 1999). For the sake of numerical ease the model sequences have been computed with older opacities (Cox & Stewart, 1970) and a mixing length parameter of $\alpha_{MLT} = 3$. While qualitatively the results presented in this paper should not be affected by this choice there are possibly details which are depending on these assumptions.

2. Decision making: no-TP, AFTP, LTP or VLTP?

The evolution of TP-AGB stars is ruled by an internal clock and the TPs which occur repeatedly after almost equidistant time intervals set the pace

at which this TP clock runs. Whether or not and to which degree an AGB star will show H-deficiency later on depends on the phase of the TP pulse cycle at which the star leaves the AGB. It defines the TP time until the next TP would occur during an undisturbed TP cycle. At this moment another clock starts to run at the pace at which the remaining envelope is reduced by H-burning and mass loss. Moreover, when the star leaves the AGB there is the He-burning clock starting as well, which measures the time until the object has become a WD and all nucleosynthesis has practically ceased. This time is always longer than the H-burning time.

The post-AGB fate of a star depends on the ratio of these three time scales. If the star leaves the AGB at an early pulse cycle phase then the TP time is much longer than the He-burning time and when the next thermal would be due the star has already become a white dwarf. This *no-TP* case is the most common. At a larger phase the TP time is shorter than the He-burning time but still larger than the H-burning time. In that case a thermal pulse (VLTP) occurs when the evolutionary path in the HRD is already directed towards the WD cooling track. In the VLTP case the He-flash convection zone is engulfing the envelope and the hydrogen in the outermost layers is mixed downwards and burned (Fig. 2, circle). If the star leaves the AGB at an even larger phase the TP time is smaller than the H-burning time. A thermal pulse (LTP) will occur and the situation will again be similar as displayed in Fig. 2. But this time the hydrogen burning shell has not yet ceased and no mixing of envelope material into the deeper layers will be possible (Iben, 1976). The surface abundance is undisturbed for another while until DUP during the Born-again evolution leads to efficient H-depletion. Finally, one more possibility leads to a chemically peculiar evolution. If the star leaves the AGB immediately after a TP (AFTP) the remaining envelope mass must be already very small. DUP during this phase then leads to H-deficiency already during the first (and in this case only) post-AGB evolution.

Thus, the post-AGB fate is determined by the interpulse phase at which the post-AGB evolution starts. This happens when mass loss has reduced the envelope mass below a core-mass dependent critical value. Therefore, the segmentation of the post-AGB evolution is a statistical process impressed by the mass loss as a function of phase.

3. Post-AGB stars suffering a very late thermal pulse

The VLTP scenario has been investigated by Iben & MacDonald (1995) with a semi-analytic treatment of burning protons as they are entering the He-flash convection zone (Fig. 2). Recently Herwig et al. (1999) have improved on this study by employing a fully coupled solution of a nucleosyn-

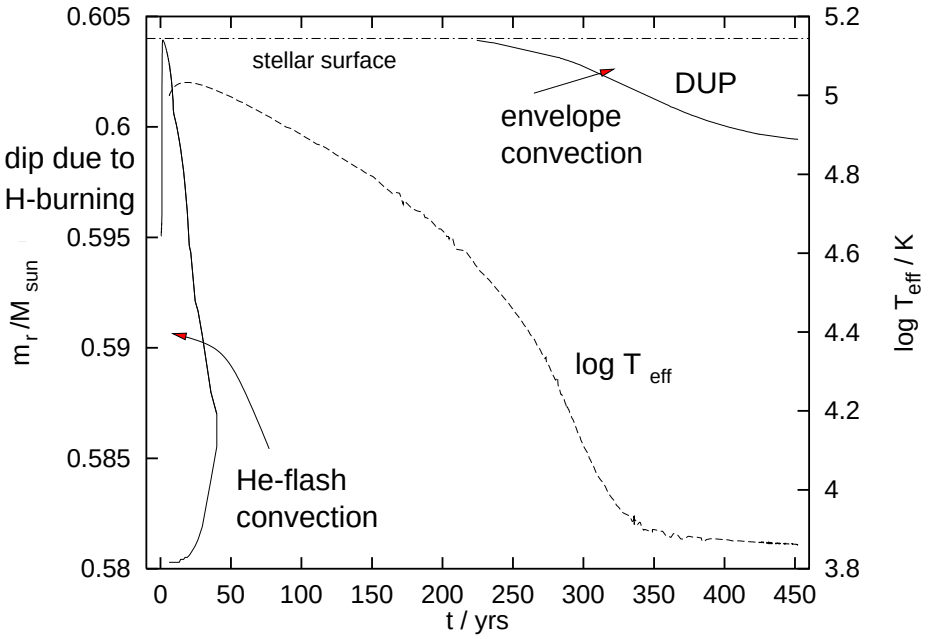

Figure 3. Internal Born-again evolution after a VLTP. The solid lines give the position of the boundaries of convection zone and the dash-dotted line indicates the position of the stellar surface (left scale). The dashed line gives the effective temperature (right scale) and shows how the model cools back into the AGB regime after the VLTP. The zero point is set to the peak He-luminosity of the pulse. The dip at the top of the He-flash convection zone at $t = 0$yr is caused by the sudden and rapid energy release from H-burning and is identical with the prominent one year long dip displayed in Fig. 2 in Herwig et al. (1999).

thesis network and a diffusion equation for each isotope. The numerical method is described in the appendix of this paper. Hydrogen is entirely destructed but no ^{14}N is produced. Instead protons ($\sim 5 \cdot 10^{-5} M_\odot$) are efficiently transformed first into ^{13}C which serves as a neutron source via the reaction chain $^{12}\mathrm{C}(\mathrm{p},\gamma)^{13}\mathrm{N}(\mathrm{e}^{+}\nu)^{13}\mathrm{C}(\alpha,\mathrm{n})^{16}\mathrm{O}$. Also we assumed that overshooting was operating in the progenitor AGB star and thereby the large oxygen mass fraction (our model: He/C/O = 0.38/0.36/0.22) observed in many H-deficient post-AGB stars has been reproduced.

Following the evolution back to the second AGB phase has revealed that Born-again AGB stars which descend from AGB models with overshoot develop a convective envelope while the outer layers are expanding and cooling. In our VLTP descendant the envelope convection develops when $\log T_{\rm eff} < 4.6$ (Fig. 3). As the star cools further envelope convection zone deepens with respect to mass, leading to **dredge-up**. We choose the term *very late dredge-up* (VLDUP) for this event because this process after

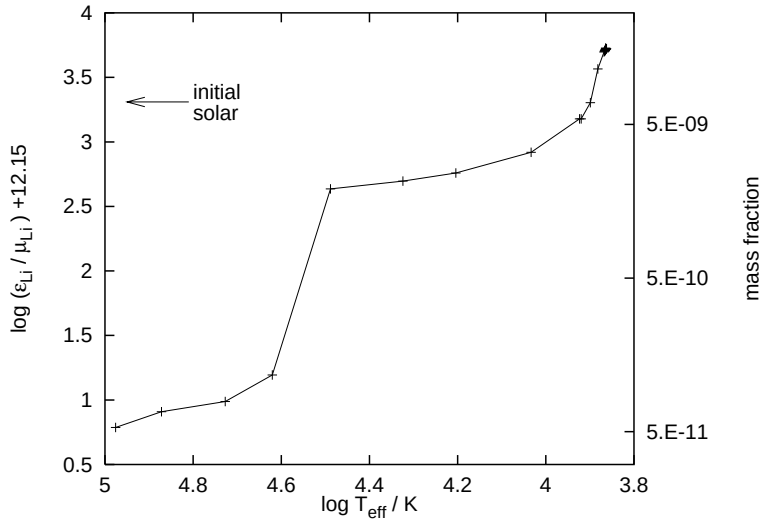

Figure 4. Evolution of lithium abundance in the convective zone below the surface during the evolution after a VLTP back to the AGB domain in the HRD (see Fig. 3).

a VLTP has distinctly different properties compared to the well known third DUP. The VLDUP has not been reported from previous model sequences evolved from AGB progenitors without overshoot. In the new models the efficient dredge-up is related to the larger TP peak He-burning luminosity due to overshoot from below the He-flash convection zone. Additionally the decreased intershell helium abundance compared to models without overshoot favours a deep envelope convection. The neutron-capture nucleosynthesis (which has not yet been followed in detail) products which will form in the He-flash convection zone after the ingestion of protons will now show up at the surface. Another effect of this VLDUP is the significant enrichment of **lithium** (Fig. 4). After a VLTP lithium is present in the intershell and mixed to the surface by dredge-up. It is the result of β-decay of ^{7}Be which has formed in the intershell by α-captures of ^{3}He. ^{3}He enters into the He-flash convection zone during the VLTP together with hydrogen from the envelope.

4. Post-AGB stars suffering a late thermal pulse

Contrary to the case of the VLTP the surface abundance remains undisturbed by the LTP itself. However, H-deficiency is caused by dredge-up during the following Born-again phase. The outer layers react to the enormous energy release by He-burning during the LTP by a very fast evolution

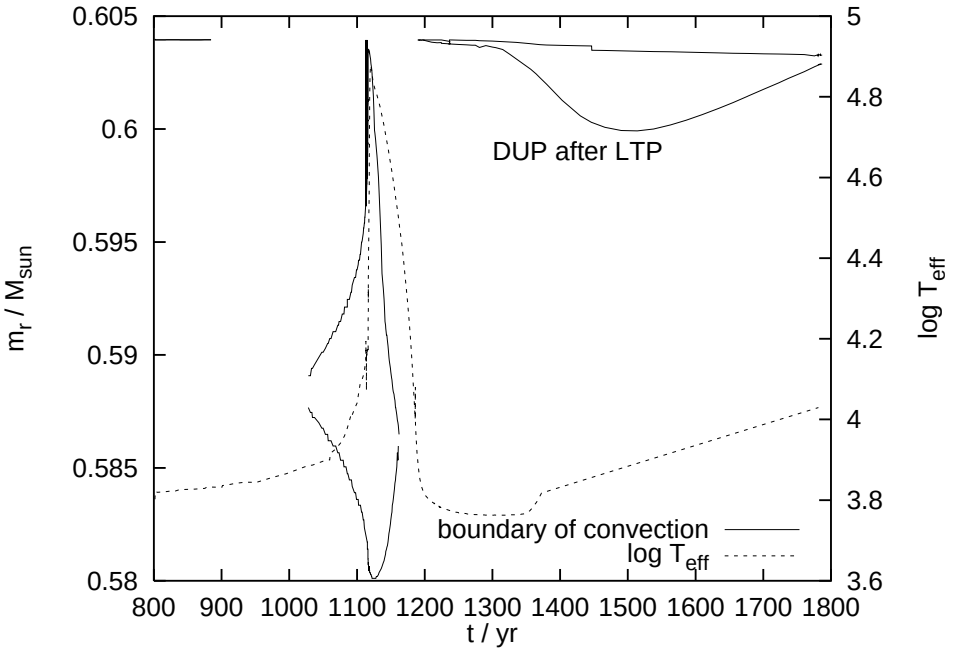

Figure 5. Internal evolution of Born-again post-AGB model sequence after a LTP.

back to the AGB. At $\log T_{\rm eff} \sim 4.0$ the outer layers become convectively unstable, similar to the previously described evolution after the VLTP (Sec. 3). The internal evolution is displayed in Fig. 5. During the coolest stage of the Born-again evolution again dredge-up is found. This *late DUP* (LDUP) does cause a substantial abundance change because the remaining envelope mass is only $< 10^{-4}{\rm M}_{\odot}$. The surface abundance evolution changes as the bottom of the envelope convection proceeds into the interior where it passes the various sites of nuclear burning (Fig. 6)[1] . Immediately after the convective zone has formed it enters into a lithium-rich region. It originates from the ^{7}Be pocket which forms due to the partial pp-chain operation at the cool side of the H-shell. Then the convective region proceeds through the fully H-burned region and a corresponding peak in the helium and nitrogen abundance can be seen in Fig. 6. Finally the dredge-up proceeds into the former intershell region. Now the intershell abundance shows up at the surface as it has been formed cumulatively over the entire previous TP-AGB evolution with overshoot. At this stage which is reached shortly

[1]Close comparison of Fig. 5 and 6 show an apparently unsynchronized behaviour of DUP and abundance change. It is related to a split of the envelope convection which probably is caused by the opacities.

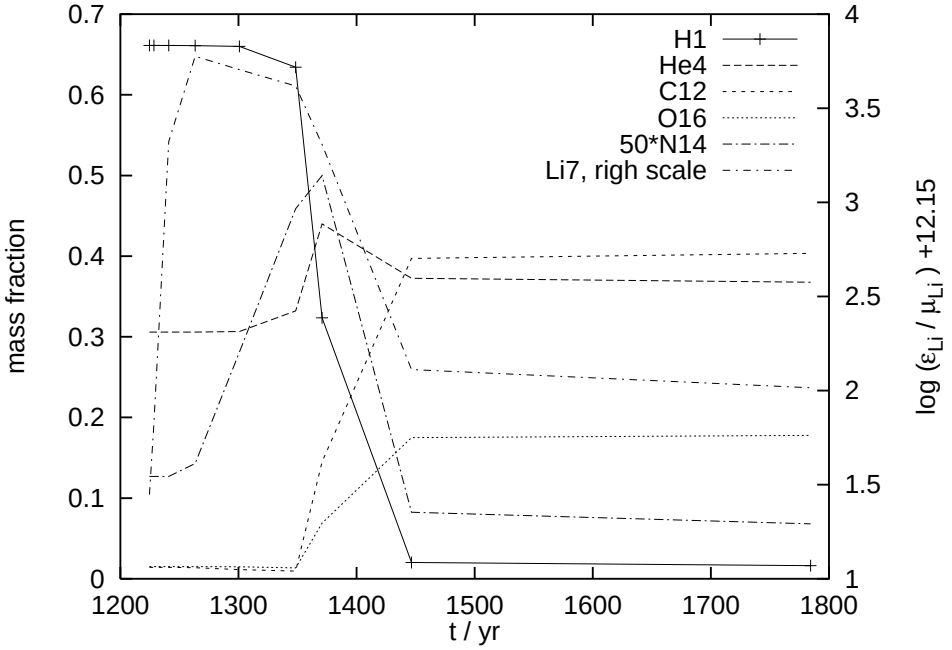

Figure 6. Surface abundance during Born-again evolution after LTP. Lithium abundance right scale.

after the lowest temperature during the Born-again evolution the surface abundances of this LTP model are $X_{\rm H} = 0.02$, $X_{\rm He} = 0.37$, $X_{\rm C} = 0.40$, $X_{\rm O} = 0.18$.

5. The AGB final thermal pulse

The third evolutionary channel also causes H-deficiency by dredge-up but this time the dredge-up occurs after the last (or final) thermal pulse on the AGB. This AFTP is characterized by a very low remaining envelope mass and it has, due to overshoot, a larger energy production by He-burning compared to models without overshoot. We have computed two AFTP cases which have been started from the same AGB model sequence as the other post-AGB tracks. The mass loss has been tuned in such a way that the envelope mass after the TP and before the succeeding DUP was $3 \cdot 10^{-2} {\rm M}_\odot$ and $4 \cdot 10^{-3} {\rm M}_\odot$ respectively (see Fig. 7 for case 1). In both cases the dredged-up mass was about $6 \cdot 10^{-3} {\rm M}_\odot$. At the end of this AGB final DUP (AFDUP) the surface abundance was $X_{\rm H} = 0.55$, $X_{\rm He} = 0.31$, $X_{\rm C} = 0.07$, $X_{\rm O} = 0.04$ in case 1 and $X_{\rm H} = 0.17$, $X_{\rm He} = 0.33$, $X_{\rm C} = 0.32$, $X_{\rm O} = 0.15$ in case 2.

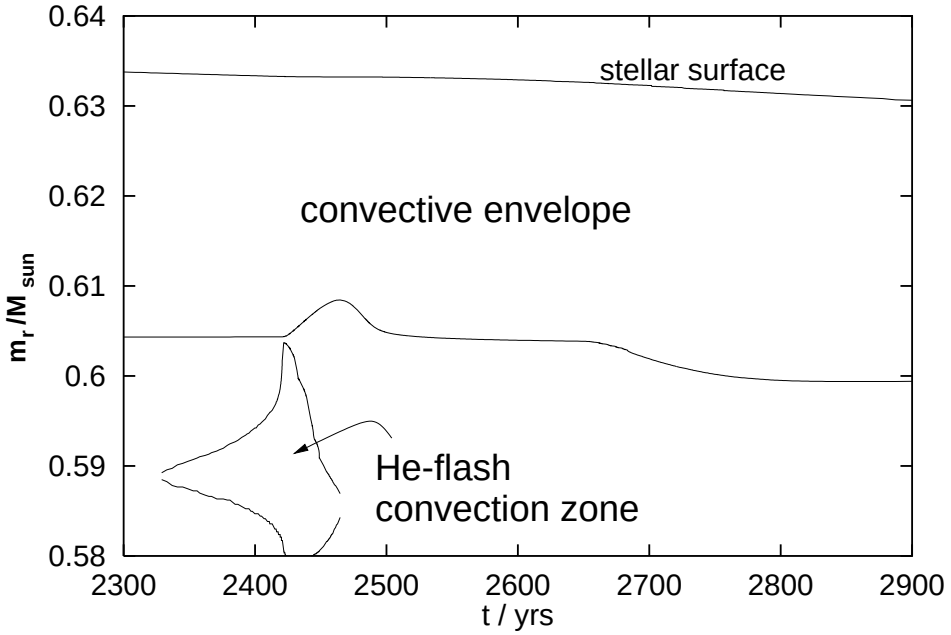

Figure 7. An AFTP model sequence: Evolution of mass coordinate of convective boundaries and stellar surface during the last TP on the AGB (see text, case 1). DUP starts at $t \sim 2670yr$.

6. Conclusions

Table 1 gives an overview of the H-abundances according to our current understanding of the formation of H-deficient post-AGB stars. The H-abundances given are most uncertain for the AFTP case because of poorly known input physics like the variation of the mass loss during the thermal pulse. If the mass loss during the final AGB interpulse period is constant and if only small modulations of the mass loss rate during and immediately after the AFTP are assumed then the rate of AFTP descendents should be only a few percent and presumably smaller than the fraction of LTP descendants which can be estimated to be somewhere between 5% and 10%. An estimate for the VLTP fraction is difficult at the moment. However, it seems that the number of 20% H-deficient post-AGB stars can not be produced from one scenario alone. Thus, it will be a future challenge to assign individual objects to a specific scenario.

For example, Sakurai's object is commonly believed to be a typical case of a Born-again star (therefore no AFTP descendant) witnessed during its rapid evolution. From our models it can currently not be in the process of

TABLE 1. Classification of post-AGB evolution, : indicates uncertain values.

Name	occurrence of H-deficiency	$X_{\rm H}$
AFTP	during 1st AGB departure	0.15 to solar (:)
VLTP	before return to 2nd AGB stage	$\leq 10^{-7}$
LTP	during 2nd AGB stage	~ 0.02

a LDUP. According to Asplund (1999) the object is in the second AGB phase, already H-deficient ($\rm X_H < 1\%$) and the H-abundance is further decreasing. At the same time the lithium abundance is increasing significantly. However, during a LDUP the Li-abundance increase is only expected during the initial phase of DUP where the star is still H-normal ($\rm X_H \sim 65\%$). The following H depletion is correlated with a lithium abundance decrease (Fig. 6) and does therefore not resemble Sakurai's object. The pattern of abundance change of this star is closer to that found during a VLDUP where the convection penetrates a zone which is H-free and Li-rich. However the observed H-abundance - although already small - is still larger by some orders of magnitude than that predicted by our current VLTP model. Maybe this inconsistency can be resolved by further investigation of VLTP models with progenitors that depart from the AGB at a slightly different interpulse phase compared to our current VLTP model.

7. Appendix: The numerical method for coupled mixing and nuclear burning

We have developed a numerical method for the fully coupled computation of mixing and nuclear burning to be used in conjunction with a stellar evolution code. It allows to follow the abundance change under conditions where the (convective) mixing time scale and the time scale of nuclear burning are of the same order of magnitude.

Mixing in convectively unstable stellar regions (Langer et al. 1985) and in the adjacent overshoot regions (Herwig et al. 1997) can be mathematically described by a diffusion equation. For each isotope i ($i = 1 \ldots i_{\rm max}$) a second order partial differential equation of the form

$$\left(\frac{\rm dX_i}{\rm dt}\right)_{\rm mix} = \frac{\partial}{\partial m}\left[\left(4\pi r^2 \rho\right)^2 D \frac{\partial X_i}{\partial m}\right] \qquad (1)$$

is set up where X_i is the abundance of isotope i, ρ density, r radius and m mass coordinate. The nuclear burning processes are defined by a set of reaction rates, the nuclear network. The time derivative of the isotope

abundances at mass grid point j can be written as

$$\left(\frac{\mathrm{d}\vec{\mathrm{X}}_\mathrm{j}}{\mathrm{dt}}\right)_\mathrm{burn} = \hat{F}_j \cdot \vec{X}_j. \tag{2}$$

The vector $\vec{X}_j$ contains the abundances of all considered isotopes at grid point j. $\hat{F}_j$ is the rate matrix which contains the functional dependence of the reaction rates on the state variables. The overall abundance change over a given time step is the sum of the contribution from mixing and from burning respectively (Eq. 1 and 2). It is discretized fully implicit for the mixing term and by a simple Euler step (likewise implicit) for the burning term. The discritized equation can be written for each grid point j:

$$\vec{X}_j^{\mathrm{n}+1} - \vec{X}_j^{\mathrm{n}} = h\hat{F}_j(\vec{X}_j^{\mathrm{n}+1}) + h[\hat{P}_j\vec{X}_{j+1}^{\mathrm{n}+1} - \hat{Q}_j\vec{X}_j^{\mathrm{n}+1} + \hat{R}_j\vec{X}_{j-1}^{\mathrm{n}+1}], \tag{3}$$

where h is the time step, n is the index numbering the time step and $\hat{P}_j$, $\hat{Q}_j$ and $\hat{R}_j$ are diagonal matrices with the diagonal elements

$$p_j = \frac{D^*_{\mathrm{j}-1}}{ml_\mathrm{j}}\frac{\Delta t}{mm_\mathrm{j}}, r_j = \frac{D^*_\mathrm{j}}{mr_\mathrm{j}}\frac{\Delta t}{mm_\mathrm{j}},$$
$$q_j = (\frac{D^*_\mathrm{j}}{mr_\mathrm{j}} + \frac{D^*_{\mathrm{j}-1}}{ml_\mathrm{j}})\frac{\Delta t}{mm_\mathrm{j}}$$
$$\text{with } ml_\mathrm{j} = m_\mathrm{j} - m_{\mathrm{j}-1},\ mr_\mathrm{j} = m_{\mathrm{j}+1} - m_\mathrm{j},$$
$$mm_\mathrm{j} = \frac{1}{2}(m_{\mathrm{j}+1} - m_{\mathrm{j}-1}) \text{ and } D^*_\mathrm{j} = \left(4\pi r^2\rho\right)^2 D_\mathrm{j}$$

at the grid point j. Neighbouring grid points are coupled by the diagonal operators $\hat{P}_j$ and $\hat{R}_j$. The discretization for the first and last grid point follows from the boundary condition of vanishing mass flux.

Equation 3 has been solved by Newton's method. For each grid point a vector function according to Eq. 3 is given by:

$$\vec{G}_j = \vec{X}_j^{\mathrm{n}+1} - \vec{X}_j^{\mathrm{n}} - h\hat{F}_j(\vec{X}_j^{\mathrm{n}+1}) - h[\hat{P}_j\vec{X}_{j+1}^{\mathrm{n}+1} - \hat{Q}_j\vec{X}_j^{\mathrm{n}+1} + \hat{R}_j\vec{X}_{j-1}^{\mathrm{n}+1}]. \tag{4}$$

The independent variable of this non-linear function is the abundance $\vec{X}^{\mathrm{n}+1}$ belonging to the time $t^{\mathrm{n}+1} = t^\mathrm{n} + h$. The grand vectors $\vec{\mathbf{G}}$ and $\vec{\mathbf{X}}^{\mathrm{n}+1}$ contain $\vec{G}_j$ and $\vec{X}_j^{\mathrm{n}+1}$ for all grid points j.

$\vec{\mathbf{X}}^{\mathrm{n}+1}$ contains a solution of Eq. 3 for each grid point $\mathbf{j}$ if

$$\vec{\mathbf{G}}(\vec{\mathbf{X}}^{\mathrm{n}+1}) = \vec{\mathbf{0}}. \tag{5}$$

Newton's method for root finding replaces the nonlinear Eq. 5 by a linear equation for the corrections $\delta\vec{\mathbf{X}}^{n+1,l}$ to the previous solution $\vec{\mathbf{X}}^{\mathrm{n}+1,\mathrm{l}}$:

$$\vec{\mathbf{G}}(\vec{\mathbf{X}}^{\mathrm{n}+1,\mathrm{l}}) + \frac{\partial\vec{\mathbf{G}}(\vec{\mathbf{X}}^{\mathrm{n}+1,\mathrm{l}})}{\partial\vec{\mathbf{X}}^{\mathrm{n}+1,\mathrm{l}}}\delta\vec{\mathbf{X}}^{\mathrm{n}+1,\mathrm{l}} = \mathbf{0}. \tag{6}$$

The initial guess may be $\vec{\mathbf{X}}^{\mathrm{n+1,l}} = \vec{\mathbf{X}}^{\mathrm{n}}$. The block tri-diagonal Jacoby matrix $\frac{\partial \vec{\mathbf{G}}(\vec{\mathbf{X}}^{\mathrm{n+1,l}})}{\partial \vec{\mathbf{X}}^{\mathrm{n+1,l}}}$ contains on its main diagonal the matrices

$$\frac{\partial \vec{G}_{\mathrm{j}}}{\partial \vec{X}_{\mathrm{j}}^{\mathrm{n+1}}} = \hat{1} - h\hat{F}_j + h\hat{Q}_j, \tag{7}$$

as well as on the upper and lower diagonal the elements

$$\frac{\partial \vec{G}_{\mathrm{j}}}{\partial \vec{Y}_{\mathrm{j+1}}^{\mathrm{n+1}}} = -h\hat{P}_j \text{ , und } \frac{\partial \vec{G}_{\mathrm{j}}}{\partial \vec{X}_{\mathrm{j-1}}^{\mathrm{n+1}}} = -h\hat{R}_j. \tag{8}$$

By recursive solution of Eq. 6 a better approximation for $\vec{\mathbf{X}}^{\mathrm{n+1}}$ can be found iteratively:

$$\vec{\mathbf{X}}^{\mathrm{n+1,l+1}} = \vec{\mathbf{X}}^{\mathrm{n+1,l}} + \delta\vec{\mathbf{X}}^{\mathrm{n+1,l}}. \tag{9}$$

For one model of the previously described VLTP sequence typically three to five iterations minimize the largest relevant relative correction with $\delta X_{\mathrm{ij}}^{\mathrm{max,rel}} < 10^{-3}$. The largest absolute corrections which usually belong to the more abundant isotopes then have the order of magnitude $\delta X_{\mathrm{ij}}^{\mathrm{max,abs}} < 10^{-6} \ldots 10^{-8}$. In the computations we found the smallest proton abundance in the burning region which can be represented to be 10^{-14} (mass fraction). With a hydrogen abundance of 10^{-14} the half life time of ^{12}C against destruction by proton capture is $\simeq 10^5$yr.

Acknowledgments: I would like to thank T. Blöcker, L. Koesterke, N. Langer and K. Werner for many very helpful discussions. This work has been supported by the *Deutsche Forschungsgemeinschaft* through grant La 587/16.

References

Asplund, M., 1999, in T. L. Bertre, A. Lebre, and C. Waelkens (eds.), AGB Stars, IAU Symp. 191, p. 481, PASP
Blöcker, T., 1995, A&A 297, 727
Cox, A. N. and Stewart, J. N., 1970, ApJS 19, 243
Fujimoto, M. Y., 1977, PASJ 29, 331
Herwig, F., Blöcker, T., Langer, N., and Driebe, T., 1999, A&A 349, L5
Herwig, F., Blöcker, T., Schönberner, D., and El Eid, M. F., 1997, A&A 324, L81
Iben, Jr., I., 1976, ApJ 208, 165
Iben, Jr., I. and MacDonald, J., 1995, in D. Koester and K. Werner (eds.), White Dwarfs, No. 443 in LNP, p. 48, Springer, Heidelberg
Langer, N., El Eid, M., and Fricke, K. J., 1985, A&A 145, 179